agronomy

MDPI

Article

Panax notoginseng–Polygonatum kingianum Rotation Alters Soil Ecoenzymatic Stoichiometry and Reduces Enzyme-Inferred Microbial Carbon Limitation in the *Pinus armandii* Understory

Yingjun Li [1,†], Jingying Hei [1,†], Yanhua Zhu [1], Rui Rui [2], Xiaoli Wan [3], Longfeng Yu [4], Biao Wang [5], Xiahong He [2], Shu Wang [1,*] and Jiansong Peng [1]

[1] College of Landscape Architecture and Horticulture, Southwest Forestry University, Kunming 650224, China; liyingjun@swfu.edu.cn (Y.L.); jyhei@swfu.edu.cn (J.H.); zhuyanhua@swfu.edu.cn (Y.Z.); pengjiansong@swfu.edu.cn (J.P.)
[2] Yunnan Provincial Key Laboratory for Conservation and Utilization of In-Forest Resource, Southwest Forestry University, Kunming 650224, China; ruirui@swfu.edu.cn (R.R.); hxh@swfu.edu.cn (X.H.)
[3] Lincang Academy of Forestry Sciences, Lincang 677099, China; wanli82127@swfu.edu.cn
[4] College of Biotechnology and Engineering, West Yunnan University, Lincang 677000, China; 2009100334@wynu.edu.cn
[5] Department of Biochemistry and Molecular Biology, School of Life Sciences, China Medical University, Shenyang 110122, China; wangbiao@cmu.edu.cn
* Correspondence: wangshu@swfu.edu.cn; Tel.: +86-871-6386-3632
† These authors contributed equally to this work.

Abstract

Long-term continuous cropping of *Panax notoginseng* (Sanqi) in the understory agroforestry systems of southwest China disrupts soil biogeochemical cycles and triggers microbial nutrient limitation. Nonetheless, it remains unclear how rotation with compatible medicinal plants regulates soil ecoenzymatic stoichiometry and enzyme-inferred microbial nutrient limitation in *Pinus armandii* understories. Here, pure *P. armandii* stands (Pa), Sanqi continuous cropping (SS), and Sanqi–*Polygonatum kingianum* rotation (SP) systems were established as three treatments in a subtropical plateau mountain region. We analyzed edaphic properties, extracellular enzyme activities, and bacterial and fungal gene abundance. The results showed that both SS and SP markedly reduced soil extracellular enzyme activities relative to the Pa control. Vector analysis indicated universal phosphorus limitation across all treatments (vector angle > 45°), with no significant difference in phosphorus limitation intensity between SS and SP. Notably, SS increased vector length and thus aggravated enzyme-inferred microbial carbon limitation, while SP effectively alleviated such carbon constraint. Seasonal variation exerted a stronger influence on soil ecoenzymatic traits and microbial nutrient limitation than planting systems. Redundancy analysis (RDA) revealed that total potassium soil organic carbon and the fungi-to-bacteria ratio were the key factors governing soil enzyme profiles in the SP system. Besides bacterial and fungal abundance, the F:B ratio, soil physical properties, soil chemical properties in the SP system also directly drove vector length. Collectively, based on one-year monitoring, SP rotation modified soil ecoenzymatic stoichiometry and reduced enzyme-inferred microbial carbon limitation in the *P. armandii* understory. These findings provide empirical evidence for optimizing medicinal plant agroforestry management in *P. armandii* forests.

Keywords: *Pinus armandii*; Sanqi continuous cropping; *Polygonatum kingianum* rotation; ecoenzymatic stoichiometry; microbial nutrient limitation; seasonal dynamics

Check for updates

Academic Editors: Cezary A. Kwiatkowski and Elżbieta Harasim

Received: 10 October 2026
Revised: 28 October 2026
Accepted: 28 October 2026
Published: 29 October 2026

Copyright: © 2026 by the authors. Licensee MDPI, Basel, Switzerland. This article is an open access article distributed under the terms and conditions of the Creative Commons Attribution (CC BY) license.

1. Introduction

Understory cultivation of *Panax notoginseng* (Sanqi) has become a vital ecological-agriculture model for sustainable production of traditional Chinese medicinal materials and has undergone rapid expansion in core producing areas, including Yunnan Province. Leveraging forest ecosystems to mimic the natural habitat of wild Sanqi, this system preserves medicinal quality while easing pressure on arable-land resources. Previous research demonstrates that understory Sanqi cultivation improves root and flower quality [1–4], enhances soil fertility and heavy-metal remediation capacity [5,6], boosts soil multifunctionality [7] and rare microbial diversity [8–10], reshapes soil metabolite profiles [11–13], and relieves microbial carbon limitation [12,14,15]. Nevertheless, this cultivation system still confronts major constraints, among which intrinsic continuous cropping obstacles and soil-borne diseases constitute two primary bottlenecks. Even though understory conditions can partially suppress disease outbreaks, root-released allelochemicals, including organic acids (e.g., oxalic and citric acids) and saponins, accumulate in rhizosphere soil [16]. These compounds trigger autotoxicity, impair root growth, and facilitate pathogen proliferation [17,18]. Without long rotation intervals (normally 10–15 years), contaminated-soil isolation, or soil amendments such as humic acid and biochar application [15], large-scale planting will accelerate soil degradation. Accordingly, developing well-designed rotation schemes compatible with understory conditions to modify edaphic properties associated with Sanqi continuous cropping carries great practical importance. Prior work has reported that using *Coix lacryma-jobi* as a preceding rotation crop markedly elevates rhizospheric abundance of *Trichoderma asperellum*, which in turn alleviates Sanqi continuous cropping obstacles. As forest understory environments exert unique environmental filtering on plant establishment and productivity, selecting suitable medicinal species for rotation with Sanqi is of great theoretical and practical significance for the green and sustainable development of its planting industry.

Changes in soil extracellular enzyme activity (EEA) and ecoenzymatic stoichiometry (EES) can effectively reflect soil biogeochemical processes and microbial nutrient status, offering critical insights into the mechanisms underlying soil degradation and the alleviation of CCOs [15]. Soil extracellular enzymes, as key products of microbial metabolism, play an indispensable role in nutrient cycling within terrestrial ecosystems [15]. By catalyzing the hydrolysis and oxidation of macromolecular organic substrates, these enzymes transform carbon (C), nitrogen (N), and phosphorus (P) into inorganic forms accessible to plants [19]. Consequently, EEA both mirrors microbial nutrient requirements and modulates soil biogeochemical cycles [20]. As a robust diagnostic framework, EES captures the constraints imposed on soil microbial energy and nutrients [21,22].

Soil EEAs exhibit substantial variation across agroforestry systems. For example, poplar–wheat and coffee–silver wattle agroforestry systems significantly enhance soil EEAs [23,24]. In contrast, systems including poplar–alfalfa, pear–konjac, and pine–Sanqi reduce these enzyme activities [15,25,26]. Such discrepancies arise from the combined controls of plant species composition, soil microbial communities, field management practices and environmental factors [15,25,27]. Likewise, different rotation regimes exert marked influences on soil EEAs. Maize–soybean rotation greatly elevates C and N cycling enzyme activities [28], whereas green manure-crop rotation substantially modifies the patterns of soil EES [29]. Rotation modulates EEA and EES primarily via three mechanisms. First, rotation stimulates enzyme production through substrate diversity: crop residues vary substantially in chemical composition, and periodic inputs of heterogeneous organic substrates induce synthesis of a broader array of extracellular enzymes [30]. Second, rotation initiates microbial community restructuring. It reshapes the taxonomic composition and functional potential of rhizosphere microorganisms, which in turn fine-tunes the synthesis and

secretion of target extracellular enzymes [31]. Third, rotation modifies microbial nutrient-limitation status: crop diversification enhances the activities of N- and P-acquiring enzymes, thereby alleviating N and P constraints [32]. Nevertheless, understory agroforestry and medicinal-plant rotation produce combined effects that complicate soil extracellular enzyme dynamics and alter plant-available resource supplies as well as microbial metabolic status. Accordingly, characterizing shifts in soil EEA and EES in the Sanqi-*P. kingianum* rotation system is essential for unpacking these intricate interactive processes.

To address these critical knowledge gaps, this study was conducted in a subtropical highland region under *P. armandii* forest, establishing three experimental treatments: pure *P. armandii* stands (Pa), Sanqi continuous cropping (SS), and Sanqi–*P. kingianum* rotation (SP) systems. We systematically measured edaphic properties, EEAs and EES, and bacterial and fungal abundances. By integrating vector analysis, redundancy analysis (RDA), and structural equation modeling (SEM), we aimed to comprehensively decipher the impacts of planting systems and seasonal dynamics on EES and microbial nutrient limitations. We hypothesized that (1) the SP rotation would reduce the exacerbated enzyme-inferred microbial C limitation caused by Sanqi continuous cropping by modulating edaphic factors and microbial abundance; and (2) both seasonal variations and planting systems would exert a direct driving effect on soil ecoenzymatic traits and microbial nutrient limitations. These results offer a scientific basis for sustainably managing and optimizing *P. armandii* understory medicinal cultivation, thereby enhancing the ecological and economic resilience of agroforestry systems.

2. Materials and Methods

2.1. Research Area and Experimental Design

The field experiment was carried out in Dadishui Village, Xundian Hui and Yi Autonomous County, Kunming, Yunnan Province, China (103°11′17″ E, 25°27′15″ N), at an elevation of 2187.5 m. The region has a typical subtropical plateau monsoon climate with well-defined dry and wet seasons. The zonal soil is classified as mountain red soil, and the local dominant native vegetation consists of *Pinus armandii* forests. In the experimental area, the *P. armandii* stands exhibited an average tree height of 9.5 m, an average diameter at breast height of 18 cm, and a canopy closure of 70%.

In this study, pure *P. armandii* stands (Pa) were used as the control, and two understory planting systems were established: a Sanqi continuous cropping system (SS) and a sequential Sanqi–*Polygonatum kingianum* rotation system (SP). The experimental plots were previously managed under a Sanqi–*P. armandii* agroforestry system, where Sanqi was cultivated from January 2020 to December 2022. Following Sanqi harvesting, the original planting ridges were retained for subsequent seedling transplantation. The ridges were standardized with a height of 40 cm, a base width of 120–150 cm, and a top width of 80–100 cm, exhibiting a wide-base and narrow-top profile. Seedlings of Sanqi and *P. kingianum* were raised in a greenhouse in January 2022. In January 2023, uniformly grown one-year-old seedlings of the two species were transplanted onto the reserved ridges of the corresponding treatments: Sanqi seedlings for SS plots, and *P. kingianum* seedlings for SP plots. The SP treatment was a sequential rotation rather than simultaneous intercropping, with *P. kingianum* planted exclusively during the experimental year. The planting spacing was set at 10–15 cm × 10–15 cm for *Panax notoginseng* and 20–30 cm × 20–30 cm for *P. kingianum*. After transplantation, the planting area was backfilled with 2–5 cm of surface soil and mulched with 3–5 cm of pine needles to conserve soil moisture [33]. All field management practices were performed consistently in accordance with the standardized methods reported [2–4].

2.2. Sampling

Rhizosphere soil sampling was performed throughout the growing season of Sanqi and *P. kingianum*. For each of the three treatments (Pa, SS, and SP), 36 (12 months × 3 replicates) independent 10 m × 10 m plots were randomly arranged, yielding a total of 108 experimental plots. Continuous monthly sampling was carried out from 20 January to 20 December 2023. Monthly samples were grouped into four seasons according to regional climate characteristics and crop growth phenology of the study area: winter (January–March), spring (April–June), summer (July–September), and autumn (October–December). Within each plot, the five-point sampling method was adopted to collect rhizosphere soil. At each sampling site, healthy, uniformly grown and disease-free plants were carefully uprooted, and rhizosphere soil was collected using the conventional root-shaking method. All subsamples from a single plot were fully blended into one composite sample (one independent biological replicate), with no pooling across different plots. In this study, a total of 108 soil samples were obtained, comprising three treatments with three biological replicates across twelve consecutive monthly sampling campaigns (3 treatments × 12 months × 3 replicates). Each season comprised 36 soil samples, collected from 3 treatments with 3 biological replicates over 3 monthly sampling events (1 sampling per month × 3 months × 3 treatments × 3 biological replicates). All soil samples were immediately transported to the laboratory and passed through a 0.149 mm sieve. The homogenized samples were then aliquoted into two subsamples: one was stored at 4 °C for the determination of edaphic properties and enzyme activities, while the other was preserved at −80 °C for microbial analysis.

2.3. Analysis of Edaphic Properties and EEAs

Soil water content (SWC) was determined gravimetrically after drying at 100 °C for 24 h. A pH meter was used to measure soil pH in a 1:5 (w/v) suspension. Total nitrogen (TN) and total phosphorus (TP) were analyzed in H_2SO_4–$HClO_4$ digests, whereas KCl extracts were used for ammonium (NH_4^+–N) and nitrate (NO_3^-–N) determination via a continuous flow analyzer (Seal Auto Analyzer AA3, SEAL Analytical, Norderstedt, Germany). Flame atomic absorption spectrophotometry (Labomed Inc., Los Angeles, CA, USA) was applied to quantify total potassium (TK). Soil organic matter (SOM) was estimated via $K_2Cr_2O_7$ oxidation, and soil organic carbon (SOC) was calculated using a conversion factor of 1.724.

The activities of seven enzymes associated with C-(xylosidase, XYL; β-1,4-glucosidase, BG; α-glucosidase, AG; cellulosic disaccharide hydrolase, CBH), N-(leucine aminopeptidase, LAP; β-1,4-N-acetylaminoglucosidase, NAG), and P-cycling (acid phosphatase, AP) were assessed using fluorometric assays. In brief, fresh soil samples (1 g) were homogenized with 125 mL of 50 mM acetate buffer (pH 5.0) via magnetic stirring. The resulting suspensions were aliquoted (150 µL) into black 96-well microplates, mixed with 50 µL of fluorogenic substrate solution to achieve a final working concentration of 200 µM per well. Substrate blanks (buffer + substrate, no soil suspension), sample blanks (buffer + soil suspension, no substrate), and quenching controls (soil suspension + standard MUB/AMC solution) were set up on the same microplate and incubated synchronously with sample wells to correct for background fluorescence and soil matrix quenching effects. Plates were incubated at 25 °C for 3 h. The reaction was terminated by adding 10 µL of 1 M NaOH to all wells, including blanks, quenching controls and standard wells, to ensure consistent pH conditions across samples, blanks and controls. Standard curves were constructed using a dilution series (0–100 µM) of 4-methylumbelliferone (MUB, for C- and P-acquiring enzymes) and 7-amino-4-methylcoumarin (AMC, for N-acquiring enzymes). Fluorescence intensity was measured using a microplate reader (Tecan Infinite M200, Salzburg, Austria) at excitation/emission wavelengths of 365/450 nm. All raw fluorescence values were first corrected by subtracting corresponding blank values, then adjusted by the quenching factor (calculated as the

ratio of standard fluorescence in pure buffer to that in soil suspension). Enzyme activity was calculated from standard curves and converted to nmol of hydrolyzed substrate per gram dry soil per hour ($nmol \cdot g^{-1} \cdot h^{-1}$) using gravimetric soil moisture content. Although two distinct fluorogenic substrates were employed (MUB for C- and P-acquiring enzymes; AMC for N-acquiring enzymes), all activities underwent identical correction workflows and were normalized to this unified unit, enabling valid cross-enzyme comparisons of hydrolytic rates.

The ecoenzymatic C:N, C:P, and N:P ratios were represented by Ln (CBH + BG + XYL + AG):Ln (NAG + LAP), Ln (CBH + BG + XYL + AG):Ln (AP), and Ln (NAG + LAP):Ln (AP), respectively. Vector angles below and above 45° indicate N and P limitations, respectively, while vector length is positively correlated with the degree of enzyme-inferred microbial C limitation [10,13,17]. The Vector length and angle were calculated as follows:

$$\text{Vector length (unitless)} = \text{SQRT}\ (x^2 + y^2) \quad (1)$$

and

$$\text{Vector angle (degrees)} = \text{Degrees}\ [\text{Atan2}\ (x,y)], \quad (2)$$

where x and y represent the ecoenzymatic stoichiometry related to C:N [Ln (CBH + BG + XYL + AG):Ln (NAG + LAP)] and C:P [Ln (CBH + BG + XYL + AG):Ln (AP)], respectively. The function Atan2 (y, x) denotes the four-quadrant inverse tangent ($\tan^{-1}(y/x)$), representing the vector angle relative to the positive *x*-axis in all plots.

2.4. Quantitative Real-Time PCR (qPCR) Analysis of Bacteria and Fungi

Total genomic DNA of soil microbes was extracted and purified using the PowerSoil DNA Isolation Kit (MoBio, St. Louis, MO, USA). The integrity of the extracted DNA was verified via 1% agarose gel electrophoresis, while DNA concentration and purity were determined using a NanoDrop 2000 spectrophotometer (Thermo Fisher Scientific, Wilmington, DE, USA). Absolute quantification of bacterial and fungal target genes was performed on a Roche LightCycler 480 II real-time PCR platform. Detailed primer information and thermal cycling procedures are provided in Table S1 of the Supplementary Materials.

Standard curves were established by ten-fold serial dilution (10^{-1} to 10^{-7}) of recombinant plasmid DNA containing the target gene fragments. The calibrated standard curves presented excellent linear fit with a coefficient of determination (R^2) higher than 0.998. The regression equations for bacterial and fungal quantification were $Y = -3.427x + 41.707$ and $Y = -3.4154x + 40.157$, respectively. To guarantee reliable and reproducible data, all qPCR amplifications were conducted in technical triplicates, and non-template controls were simultaneously set to monitor potential contamination. Melting curve analysis was applied to confirm the amplification specificity, and the amplification efficiency was maintained within the acceptable range of 90–110% for valid quantitative analysis. Absolute abundances of bacterial and fungal genes were determined from standard curves and reported as copies g^{-1} dry soil [6,7,10].

2.5. Data Statistics

Raw data were screened for normality and homogeneity of variance prior to analysis. One- and two-way ANOVA were performed in SPSS 20.0 to assess the effects of planting pattern and season on edaphic properties, microbial gene abundance, EEAs, and EES. To maintain a consistent statistical framework for error estimation across seasonal and annual scales, we averaged observations separately for the first, second, and third replicates across the three months within each season to yield three seasonal replicate means for subsequent error analysis. Partial eta-squared (η_p^2) was calculated as the effect-size metric

to quantify the relative magnitude of each factor. Least significant difference (LSD) and Duncan's tests were used for post hoc comparisons at $p < 0.05$. Origin 20.0 was used for correlation analysis among soil environmental factors, EEAs, and vector length and angle for plotting all figures. Redundancy analysis (RDA) was conducted on the OECloud platform (https://cloud.oebiotech.com) to identify the key drivers of soil EEAs across planting systems. SEM was further built to evaluate the direct and indirect effects of edaphic properties, bacterial and fungal gene abundance, and the fungi-to-bacteria (F:B) ratio on microbial nutrient limitation (vector length and angle) under the three treatments. Models were considered acceptable when $\chi^2/df < 3$, GFI > 0.6, and RMSEA < 0.1; all three treatments met these criteria (Pa: $\chi^2/df = 2.26$, GFI = 0.91, RMSEA = 0.10; SS: $\chi^2/df = 1.83$, GFI = 0.92, RMSEA = 0.04; SP: $\chi^2/df = 1.41$, GFI = 0.95, RMSEA = 0.07). Two-way ANOVA with effect size (η_p^2) was used to quantify the independent and interactive effects of planting systems and season on EEAs and vector characteristics.

3. Results

3.1. Seasonal Dynamics of EEAs and Their Stoichiometric Characteristics

Under different planting systems, EEAs exhibited significant seasonal fluctuations (Figure 1). Overall, EEAs in the SS and SP systems were significantly lower than those in the Pa system. Across all seasons, EEAs peaked in spring and winter and declined in summer and autumn (Figure 1). The total EEA magnitude followed the order of Pa > SS > SP, among which AP exhibited the highest individual activity among the seven enzymes.

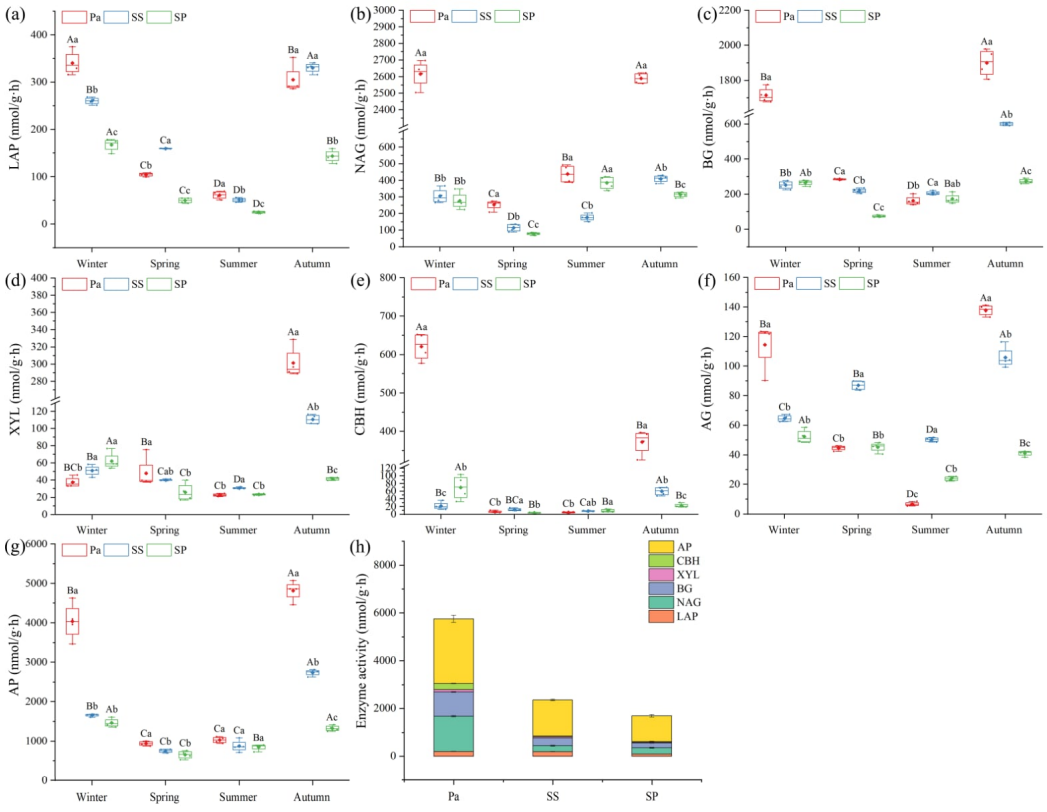


Figure 1. Seasonal dynamics of soil extracellular enzyme activities (EEAs) under three planting systems. Treatments: Pa, pure *P. armandii* stands; SS, Sanqi continuous cropping system; SP, Sanqi–*Polygonatum kingianum* rotation system. Panels (**a**–**g**) show the seasonal dynamics of seven target extracellular enzymes, respectively: (**a**) LAP, (**b**) NAG, (**c**) BG, (**d**) XYL, (**e**) CBH, (**f**) AG, and (**g**) AP. Panel (**h**) presents the annual mean EEAs across the three planting systems. Lines in the boxes

represent the medians, the top and bottom edges of the boxes represent the first and third quartiles, respectively, and the whiskers extend to 1.5 times the interquartile range; dots represent single observations. Each season included 36 soil samples (1 sampling/month × 3 months × 3 treatments × 3 biological replicates). Different lowercase and uppercase letters denote significant differences among treatments within the same season and treatment, respectively ($p < 0.05$; LSD and Duncan's tests).

The C:N:P stoichiometry ratios deviated substantially from the global average soil threshold of 1:1:1 across all three treatments, indicating divergent microbial nutrient limitation patterns. The corresponding stoichiometric ratios were 1:1.05:1.18 for Pa, 1:1.00:1.19 for SS, and 1:1.02:1.22 for SP (Figure 1 and Table S2). Relative to the Pa treatment, both SS and SP systems showed significantly higher C:N ratios and lower N:P ratios. Additionally, a notable reduction in the C:P ratio was observed in the SP system (Figure 2 and Table S2).

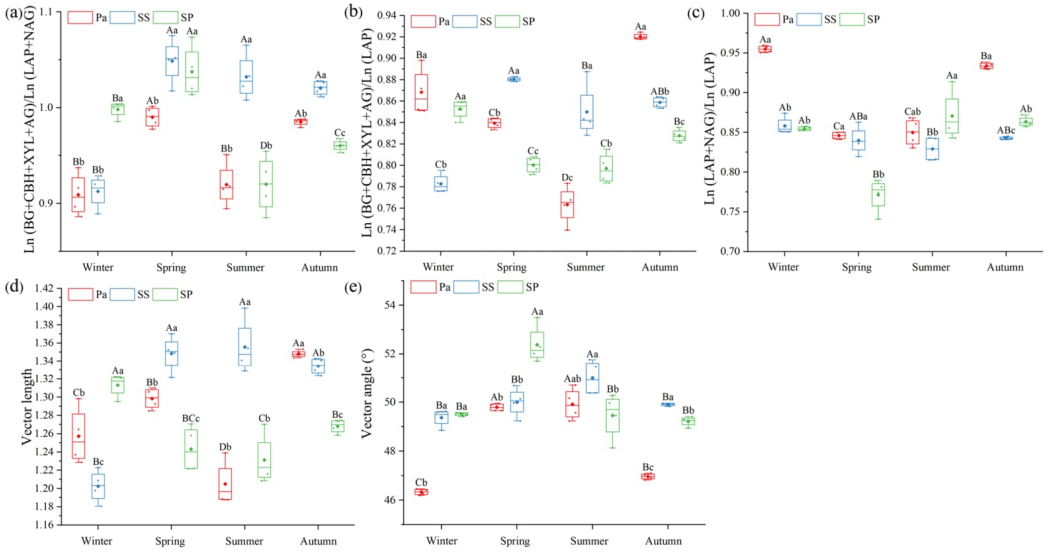


Figure 2. Seasonal dynamics of ecoenzymatic stoichiometry (EES), vector length and vector angle under three planting systems. Panels: (**a**) ecoenzymatic C:N ratio; (**b**) ecoenzymatic C:P ratio; (**c**) ecoenzymatic N:P ratio; (**d**) vector length; (**e**) vector angle. Each season included 36 soil samples (1 sampling/month × 3 months × 3 treatments × 3 biological replicates). Different lowercase and uppercase letters denote significant differences among treatments within the same season and treatment, respectively ($p < 0.05$; LSD and Duncan's tests).

Vector analysis further revealed distinct microbial nutrient limitation characteristics among treatments. The SS system exhibited the maximum vector length (1.31), which was significantly higher than those of Pa (1.28) and SP (1.26) systems, suggesting the strongest carbon limitation in SS soil. In comparison, the SP system had the shortest vector length, indicating relatively weak carbon limitation. Notably, the vector angles of all treatments exceeded 45°, ranging from 48.25° to 50.14°, demonstrating that soil microorganisms under all three planting systems were predominantly constrained by P limitation (Figure 1 and Table S2).

3.2. Responses of Edaphic Properties and Microbial Abundance

Different planting patterns significantly altered edaphic properties and microbial abundance (Tables S2–S4). Compared with the Pa system, both SS and SP systems significantly increased SOC, NH_4^+–N and NO_3^-–N, TP, WC, and soil C:N ratio, along with significantly lower TK, ST, and soil N:P ratio. Notably, TN content increased significantly in the SS system but decreased dramatically in the SP system.

With respect to microbial abundance, bacterial gene copy number was highest in the SP system (4.90×10^{10}), significantly exceeding that in the SS (2.90×10^{10}) and Pa (1.50×10^{10})

systems. In contrast, fungal gene copy number was highest in the Pa treatment (7.71×10^8), significantly higher than in the SS (2.39×10^8) and SP (2.21×10^8) systems. Accordingly, the F:B ratio was highest in the Pa system (0.051), significantly greater than in the SS (0.008) and SP (0.005) systems. These results indicate that the Pa system is characterized by a higher relative fungal abundance, whereas the SS and SP systems exhibit a distinctly bacterial-dominated microbial community.

3.3. RDA and Main Effect Analysis

The RDA results revealed that the key environmental drivers of EEAs varied markedly across the different planting systems. In the Pa system, EEAs were primarily governed by pH, TP, and SOC. In the SS system, the dominant drivers shifted to ST, the F:B ratio, and WC. Conversely, EEAs in the SP system were mainly driven by TK, SOC, F:B ratio, and ST (Figure 3 and Table S5). Furthermore, main effect analysis demonstrated that seasonal variation was the predominant factor regulating EEAs, enzymatic stoichiometry, and microbial nutrient limitation (indicated by vector length and angle), with planting system exerting a secondary but significant influence (Figure 4 and Table S6).

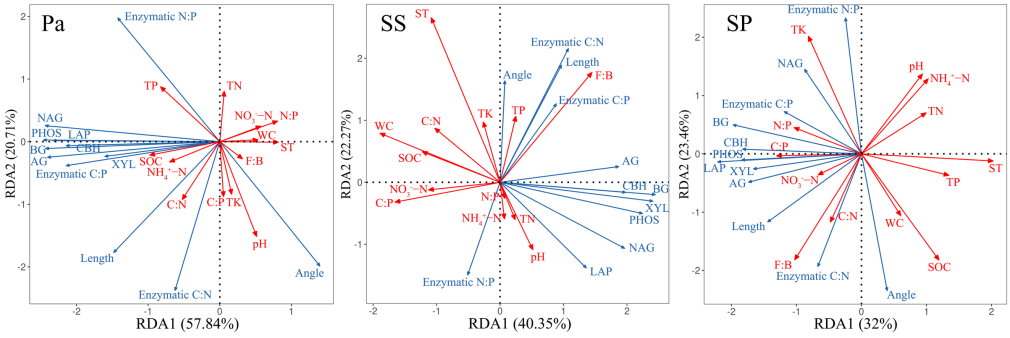


Figure 3. RDA analysis of soil enzymes and edaphic properties. Red vectors represent edaphic properties, and blue vectors represent enzyme activities.

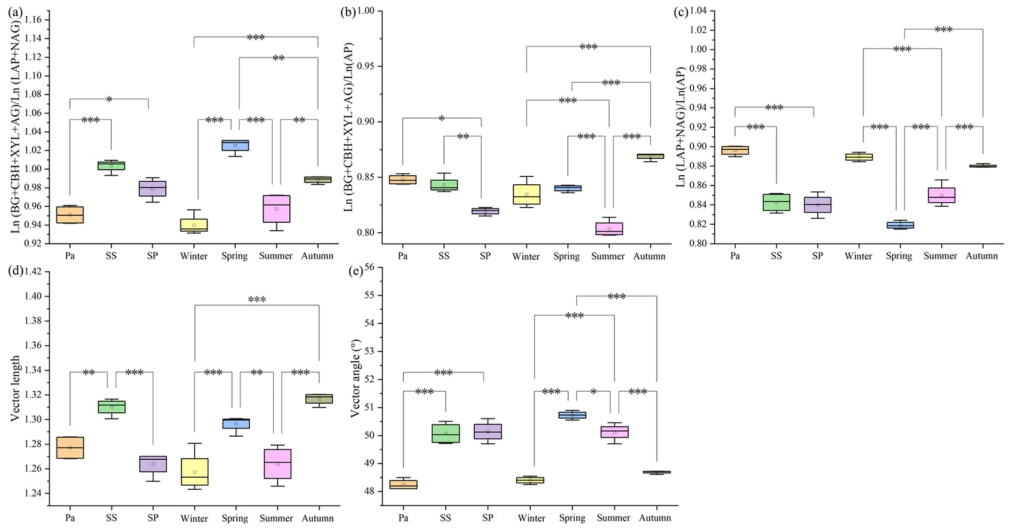


Figure 4. Effects of season, systems and their interaction on (**a**) ecoenzymatic C:N ratio; (**b**) ecoenzymatic C:P ratio; (**c**) ecoenzymatic N:P ratio; (**d**) vector length; (**e**) vector angle. Each season included 36 soil samples (1 sampling/month × 3 months × 3 treatments × 3 biological replicates). * $p < 0.05$, ** $p < 0.01$, *** $p < 0.001$.

3.4. Structural Equation Modeling (SEM)

SEM analysis revealed that in the Pa soil, the F:B ratio and soil physical properties had significant positive direct effects on vector length (Figure 5; Table S7). In contrast, the

direct drivers of vector length in the SS and SP soils were more complex. In addition to bacterial and fungal gene copy numbers, the F:B ratio, and soil physical properties, soil chemical properties in the SP system also exhibited a direct driving effect on vector length. Standardized total effect analysis further demonstrated that soil physical properties were the strongest predictors of vector length variation across all systems, followed by the F:B ratio (Figure 5 and Table S7). This indicates that under different planting systems, the improvement of the soil physical environment and the adjustment of microbial community structure (particularly changes in fungal proportion) are key drivers in alleviating or exacerbating enzyme-inferred microbial C limitation (as characterized by vector length).

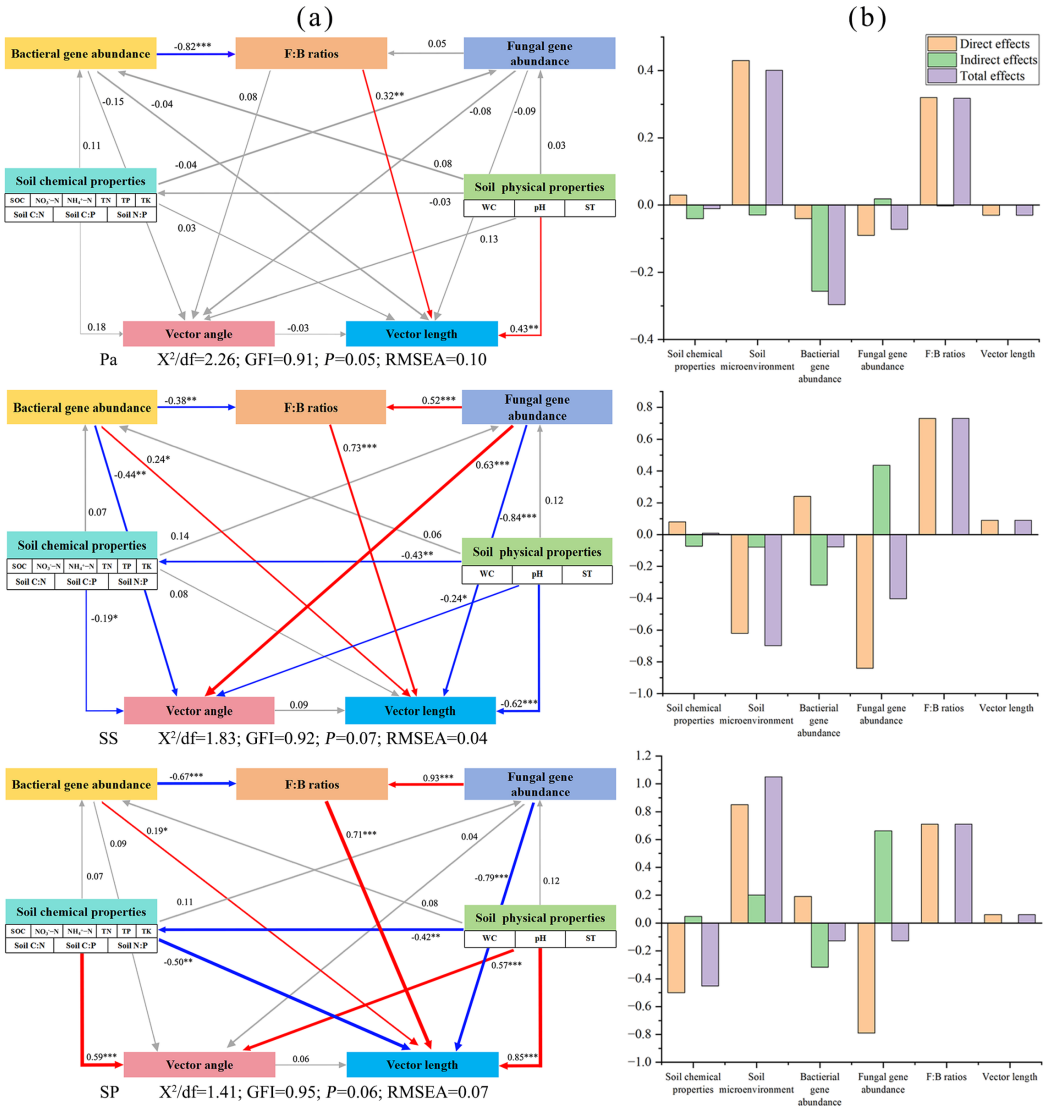


Figure 5. (**a**) Analysis of the SEM and standardized effects under different systems. Solid red and blue arrows represent significant positive or negative paths. Values on arrows show standardized path coefficients (* $p < 0.05$; ** $p < 0.01$; *** $p < 0.001$). (**b**) Standardized direct, indirect and total effects of each latent variable on enzyme-inferred microbial metabolic limitation (vector length and vector angle).

4. Discussion

4.1. Variations in EEAs Across Different Planting Systems

EEA and EES are critical biogeochemical indicators for characterizing microbial metabolic limitation, nutrient-cycling efficiency, and community responses to environmental conditions [34,35], which can directly reflect relative microbial demands for C, N,

and P and microbial nutrient-limitation status [36]. Our results showed that both SS and SP systems significantly reduced soil EEAs compared with the Pa system. Our results align with previous findings in agroforestry systems, including poplar–alfalfa, pear–konjac, and pine–Sanqi [15,25,26] but contradict observations from poplar–wheat and coffee-silver wattle agroforestry systems [23,24]. Such discrepancies are mainly attributed to the combined effects of plant species composition, soil microbial communities, field management practices and environmental factors [15,25,37]. In particular, field management practices during Sanqi and *P. kingianum* cultivation under the forest understory, including soil tillage, organic fertilizer application, and the prohibition of synthetic pesticides and chemical fertilizers, can substantially improve soil fertility [6,38], increase microbial diversity [8–10], and promote soil multifunctionality [7], which in turn contribute to the reduction in EEAs.

4.2. Microbial Nutrient-Limitation Patterns Revealed by Ecoenzymatic Vector Analysis

According to the "resource allocation strategy," soil microorganisms alleviate nutrient limitations by upregulating the synthesis of specific EEAs targeting scarce elements during organic matter decomposition [39,40]. Vector analysis revealed widespread enzyme-inferred microbial P limitation across all three treatments, suggesting that P deficiency acts as an inherent environmental filter in this subtropical alpine red soil ecosystem. However, the degree of enzyme-inferred P limitation showed no significant difference between the SS and SP systems, suggesting that *P. kingianum* rotation failed to alleviate this pervasive P constraint. This outcome may be attributed to the regional nutrient limitation context; subtropical forests in Yunnan Province, particularly pine forests, generally face severe N and P limitations [41], making it difficult for a single rotation measure to overcome the inherent P limitation pattern of the soil. By contrast, the SS system markedly increased vector length, indicating aggravated enzyme-inferred microbial C limitation. This can be explained by the continuous release of allelochemicals such as organic acids and saponins from Sanqi roots, which inhibits microbial extracellular enzyme synthesis and secretion [17]. Meanwhile, continuous input of root exudates reshapes rhizosphere resource conditions and weakens microbial carbon-acquisition capacity [14]. Importantly, the SP rotation system effectively reduced enzyme-inferred microbial C limitation. Rotation alters substrate availability via differences in chemical composition of crop residues and root exudates [30]. Accordingly, we infer that the introduction of *P. kingianum* modified rhizosphere organic-substrate inputs and improved microbial carbon-acquisition capacity, thereby relieving enzyme-inferred microbial C limitation induced by Sanqi continuous cropping.

4.3. Seasonal Effects on EEA Traits and Microbial Nutrient Limitation

Existing studies have demonstrated that climate change and land-use patterns reshape microbial nutrient-limitation patterns by altering biotic and abiotic factors. Alleviated C limitation is frequently accompanied by aggravated N or P limitation, and such trade-offs are widely observed across diverse terrestrial ecosystems [42]. Consistent with our second hypothesis, seasonal variation was identified as the primary determinant of microbial nutrient limitation, followed by the planting system. Specifically, EEAs and vector length within the SP system were significantly lower in summer and autumn but higher in spring and winter; this seasonal pattern differs from reports for other soil types [43,44]. Moreover, vector length exhibited a significant negative association with ST, while showing a positive correlation with SWC. These correlations are likely associated with seasonal alternations between dry and wet seasons in subtropical forests, which trigger large fluctuations in soil temperature and moisture. Seasonal shifts in temperature and moisture modify soil physicochemical properties and further regulate the expression level of soil extracellular enzymes [45]. RDA analysis revealed that TK and SOC were major factors governing EEAs

and EES. Additionally, the quantity and quality of plant-derived substances entering soil vary with seasons, which modifies microbial nutrient-use efficiency and ultimately regulates EEAs and their stoichiometric characteristics [46].

4.4. Edaphic Factor and Microbial Drivers of EEA Characteristics Under Sanqi-P. kingianum Rotation System

Plant introduction and crop rotation in agroforestry systems have been identified as key modulators of EEA and EES [28,47], mainly by altering edaphic properties [28,48] and soil microbial community structure [47]. RDA and SEM further illustrated that in the SP system, vector length exhibited significant inverse relationships with NH_4^+–N, TN, TP, TK and pH, with relatively high concentrations of NH_4^+–N and TP. As a readily available nitrogen source, NH_4^+–N reshapes microbial metabolic strategies and modulates coupled C and N cycling [49]. It directly alleviates intense microbial nitrogen demand, prompting a reallocation of metabolic resources from N-acquiring to C-acquiring enzymes, thereby mitigating enzyme-inferred microbial C limitation [50]. Meanwhile, elevated soil TP can markedly decrease ecoenzymatic C:P ratios, and such stoichiometric shifts usually signal a transition from P limitation toward C limitation [51]. In our study, SP soils exhibited significantly reduced ecoenzymatic C:P ratios and increased C:N ratios. These stoichiometric shifts aligned with increased soil TP concentrations, suggesting that altered soil environmental conditions enhanced microbial C use efficiency, thereby indirectly mitigating the microbial C limitation exacerbated by Sanqi continuous cropping [52].

On the other hand, bacteria and fungi exhibit distinct functional differentiation in response to environmental perturbation [53]. Their abundances show nonlinear relationships with specific enzyme activities, which are strongly dependent on the stoichiometric balance of C, N, and P [36,38]. Vector length was negatively correlated with fungal abundance but positively correlated with bacterial abundance and the F:B ratio in the SP system. Soil EEA depends not only on the abundance of enzyme-producing microorganisms but is also tightly controlled by enzyme synthesis costs, substrate availability, and product-mediated feedback inhibition [54]. Under relatively nutrient-rich conditions, microorganisms may down-regulate the synthesis of high-cost enzymes to optimize metabolic efficiency. Consequently, specific hydrolase activities can decrease substantially even when microbial abundance remains high [54]. Furthermore, different microbial groups contribute unequally to enzyme synthesis: fungi predominantly decompose recalcitrant organic matter (e.g., lignin and cellulose), with their hyphal networks secreting abundant oxidative and cellulolytic enzymes, whereas bacteria drive the rapid turnover of labile organic matter and mainly secrete hydrolases such as amylase and sucrase [55,56]. We speculate that the regulation of EEA in the SP system relies more on the restructuring of the microbial functional community than on simple increases in bacterial or fungal abundance.

5. Conclusions

In this study, we investigated how Sanqi-*P. kingianum* rotation shapes soil ecoenzymatic stoichiometry and microbial nutrient limitation under *P. armandii* understory conditions based on one-year monthly rhizosphere soil monitoring. Our results demonstrated that both Sanqi continuous-cropping (SS) and Sanqi-*P. kingianum* rotation system (SP) significantly reduced soil EEAs compared with the pure *P. armandii* stand (Pa). Vector analysis revealed widespread P limitation across all three planting systems, indicating that the soil microbial community is under persistent relative P limitation in this subtropical plateau mountain red-soil ecosystem, which cannot be relieved merely by medicinal-plant rotation. Crucially, the SS system increased vector length and thereby aggravated enzyme-inferred microbial C limitation, whereas the SP rotation system substantially alleviated this constraint, confirming

our first hypothesis. Seasonal variation exerted stronger effects than planting systems on ecoenzymatic traits and microbial nutrient limitation, supporting our second hypothesis. RDA and SEM further illustrated that soil chemical properties, soil physical properties, microbial abundance and the fungi-to-bacteria (F:B) ratio jointly governed enzyme-inferred microbial C limitation in the SP system. Collectively, the SP rotation altered soil ecoenzymatic properties and reduced enzyme-inferred microbial carbon limitation in the *P. armandii* understory based on one-year monitoring. These short-term observations point to its potential for understory medicinal-plant agroforestry management. Nevertheless, our one-year dataset cannot confirm persistent rotation effects or complete recovery from long-term continuous-cropping obstacles. Although nutrient limitations (low soil N and K together with widespread P limitation) were detected across treatments, our experiment included no fertilization trials to test whether nutrient amendments would deliver functional benefits. Accordingly, future multi-year and multi-site investigations are required to validate the long-term practical performance of this rotation system.

Supplementary Materials: The following supporting information can be downloaded at: https://www.mdpi.com/article/10.3390/agronomy16212130/s1. Table S1: The primers sequences of 16rRNA and ITS; Table S2: Analysis of soil extracellular enzyme stoichiometry; Table S3: Variations of edaphic properties and microbial copy numbers; Table S4: Seasonal variations of edaphic properties and microbial copy numbers; Table S5: RDA analysis of soil enzymes and edaphic properties; Table S6: Effects of season, treatment and their interaction on soil enzyme activities; Table S7: Correlation analysis of vector length and angle with edaphic properties and microbial copy numbers in different systems; Figure S1: Monthly dynamics of edaphic properties; Figure S2: Monthly dynamics of soil extracellular enzyme activities and enzymatic stoichiometry vector characteristics; Figure S3: Annual dynamics of soil fungal abundance, bacterial abundance and F:B ratios.

Author Contributions: Conceptualization, X.H., S.W. and J.P.; data curation, Y.Z., R.R. and X.W.; formal analysis, Y.L., J.H., L.Y. and B.W.; funding acquisition, J.H., X.H., S.W. and J.P.; investigation, Y.Z., R.R., X.W., L.Y. and B.W.; methodology, Y.Z., R.R., X.W., L.Y. and B.W.; project administration, X.H., S.W. and J.P.; resources, Y.Z., R.R., X.W., L.Y. and B.W.; software, Y.L., J.H. and R.R.; supervision, J.H., S.W. and J.P.; validation, Y.Z., R.R. and X.W.; visualization, Y.L., J.H., X.H., S.W. and J.P.; writing—original draft preparation, Y.L. and J.H.; writing—review and editing, Y.L., J.H., S.W., X.H. and J.P. All authors have read and agreed to the published version of the manuscript.

Funding: This research was supported by Yunnan Fundamental Research Projects (202601BD070001-029; 202601AS070012; 202501BD070001-023; 202501BD070001-087; 202401BD070001-122), Yunnan Provincial Key Laboratory (202402AN360005), Yunnan Province Innovation Team (202405AS350027), China Agriculture Research System of MOF & MARA (CARS-21-05B), "Xinglin Talent" Support Program (Science and Technology Special Project) (LCXLRC2025A-02), Postgraduate Scientific Research Innovation Fund of Southwest Forestry University (YJS-KCJJ-2025-10).

Data Availability Statement: The original contributions presented in this study are included in the article/Supplementary Materials. Further inquiries can be directed to the corresponding author.

Conflicts of Interest: The authors declare no conflicts of interest.

References

1. Wang, C.Y.; Mao, G.M.; Li, Y.B.; Zi, W.J.; Wang, Q.Y.; Huang, H.C.; Yang, M.; Du, F.; Mei, X.Y.; Deng, W.P.; et al. Tree Root-Mediated Soil Metabolome in Agroforestry Enhancing the Growth and Quality of *Panax notoginseng*. *Plant Soil* **2024**, *507*, 497–518. [CrossRef]
2. Sriariyanun, C.; Kunwadee, C.; Samarakoon, M.; Thinzar, S.; Win Lin, M. Phytochemical Insights and Medicinal Potential of *Panax notoginseng*: A Comprehensive Study from Chiang Mai. *Int. J. Clin. Invent. Med. Sci.* **2024**, *6*, 18–26. [CrossRef]
3. Li, Y.; Hei, J.Y.; Peng, J.S.; Zhao, X.Y.; Rui, R.; Wang, B.; He, X.H.; Wang, S. Unveiling the Molecular Regulations of Terpenoid Biosynthesis in Sanqi Flowers across Two Cultivation Systems and Flowering Stages Using Multiomics Approaches. *Ind. Crops Prod.* **2025**, *236*, 122074. [CrossRef]

4. Yang, K.; Wang, H.L.; Luo, L.F.; Zhu, S.S.; Huang, H.C.; Wei, Z.X.; Zhu, Y.Y.; Guo, L.W.; He, X.H. Effects of Different Soil Moisture on the Growth, Quality, and Root Rot Disease of Organic *Panax notoginseng* Cultivated under Pine Forests. *J. Environ. Manag.* **2023**, *329*, 117069. [CrossRef]
5. Huang, Z.G.; Shen, Z.D.; Liu, C.L.; Shi, H.N.; He, S.R.; Long, G.Q.; Deng, W.P.; Yang, J.L.; Fan, W. Characteristics of Heavy Metal Accumulation and Risk Assessment in Understory *Panax notoginseng* Planting System. *Environ. Geochem. Health* **2022**, *45*, 9029–9040. [CrossRef]
6. Hei, J.Y.; Rui, R.; Wang, S.; He, X.H. Carbon-Fixing Bacterial Network Complexity Mediates Soil Multifunctionality in a *Panax notoginseng*-*Pinus armandii* Agroforestry System. *Land Degrad. Dev.* **2026**, *37*, 10835–10850. [CrossRef]
7. Hei, J.Y.; Dong, Q.Q.; Li, Y.J.; Rui, R.; He, X.H.; Wang, S. Coupled Regulation Effects of Sanqi-Pine Intercropping Systems on Soil Fertility and Heavy Metals Mediated by Ammoniaoxidizing Microorganisms. *BMC Plant Biol.* **2026**, *26*, 1190. [CrossRef]
8. Yao, L.L.; Kong, L.; Yang, Q.L.; Nian, H.J.; Liang, J.P. Analysis of Microbial Diversity in Rhizosphere Soil of *Panax notoginseng* under Different Water and Microbial Fertilizer Conditions. *Agronomy* **2024**, *14*, 922. [CrossRef]
9. Zhao, L.Y.; Xu, W.M.; Guan, H.L.; Wang, K.Y.; Xiang, P.; Wei, F.G.; Yang, S.Z.; Miao, C.P.; Ma, L.Q. Biochar Increases *Panax notoginseng*'s Survival Under Continuous Cropping by Improving Soil Properties and Microbial Diversity. *Sci. Total Environ.* **2022**, *850*, 157990. [CrossRef]
10. Hei, J.Y.; Li, Y.; Rui, R.; He, S.; Wang, B.; Wang, S.; He, X.H. Rare Microbial α-diversity and Network Complexity Significantly Enhance Soil Multifunctionality in *Pinus armandii* under Sanqi-pine Agroforestry System. *Ind. Crops Prod.* **2026**, *243*, 123108. [CrossRef]
11. Haq, M.Z.U.; Bai, Z.Q.; Gu, G.T.; Liu, Y.; Yang, D.M.; Yang, H.G.; Yu, J.; Wu, Y.G. Continuous Cropping Obstacles in Medicinal Plants: Driven by Soil Microbial Communities and Root Exudates. A review. *Plant Sci.* **2025**, *359*, 112686. [CrossRef]
12. Liu, Z.X.; Gu, H.D.; Hu, X.J.; Yu, Z.H.; Li, Y.S.; Jin, J.; Liu, X.B.; Liu, J.J.; Wang, G.H. Enhancing Microbial Carbon Use Efficiency in Organic Rice Farming through Improved Soil Nutrient Availability and Microbial Resource Acquisition Strategies. *Agric. Ecosyst. Environ.* **2026**, *397*, 110097. [CrossRef]
13. Tuo, Y.F.; Luo, X.Q.; Wang, Z.Y.; Liang, J.P.; Shi, R.; Wang, Z.X.; Wang, S.; Xiang, P.; Yang, Q.L.; He, X.H. Effects of Water and Fertilizer Regulation on Soil Microbial Community, Fruit Nutrients, and Saponin Content of *Panax notoginseng*: A Three Years Field Experiment. *Ind. Crop Prod.* **2024**, *220*, 119166. [CrossRef]
14. Liu, Y.P.; Wang, Y.; Tian, G.B.; Yang, S.C.; Chen, J.W.; Zi, S.H.; Fan, W.; Ma, Q.R.; Liu, J.M.; Zhang, Z.; et al. *Panax notoginseng* Planted Under Coniferous Forest: Effects on Soil Health and the Soil Microbiome. *Forests* **2024**, *16*, 2. [CrossRef]
15. Liu, L.; Wu, J.H.; Liu, M.P.; Wang, M.L.; Huo, Y.W.; Wei, F.G.; Wu, M. Microbial Communities in Continuous *Panax notoginseng* Cropping Soil. *Agronomy* **2025**, *15*, 486. [CrossRef]
16. Abubakar, A.S.; Wu, Y.; Chen, F.; Zhu, A.; Chen, P.; Chen, K.; Qiu, X.; Huang, X.; Zhao, H.; Chen, J.; et al. Comprehensive Analysis of WUSCEL-Related Homeobox Gene Family in Ramie (*Boehmeria nivea*) Indicates Its Potential Role in Adventitious Root Development. *Biology* **2023**, *12*, 1475. [CrossRef]
17. Hei, J.Y.; Wang, S.; He, X.H. Effects of Exogenous Organic Acids on the Growth, Edaphic Factors, Soil Extracellular Enzymes, and Microbiomes Predict Continuous Cropping Obstacles of *Panax notoginseng* from the Forest Understorey. *Plant Soil* **2023**, *503*, 105–122. [CrossRef]
18. Wang, F.Y.; Zhan, P.; Zhang, X.M.; Xia, P.G.; Liang, Z.S. Unraveling Rotational Remedies: Deciphering the Autotoxicity of *Panax notoginseng* Saponins. *Ind. Crops Prod.* **2023**, *206*, 117601. [CrossRef]
19. Yao, X.H.; Min, H.; Lv, Z.H.; Yuan, H.P. Influence of Acetamiprid on Soil Enzymatic Activities and Respiration. *Eur. J. Soil Biol.* **2006**, *42*, 120–126. [CrossRef]
20. Luo, L.; Meng, H.; Gu, J.D. Microbial Extracellular Enzymes in Biogeochemical Cycling of Ecosystems. *J. Environ. Manag.* **2017**, *197*, 539–549. [CrossRef]
21. Cui, Y.X.; Fang, L.C.; Guo, X.B.; Wang, X.; Zhang, Y.J.; Li, P.F.; Zhang, X.C. Ecoenzymatic Stoichiometry and Microbial Nutrient Limitation in Rhizosphere Soil in the Arid Area of the Northern Loess Plateau, China. *Soil Biol. Biochem.* **2018**, *116*, 11–21. [CrossRef]
22. He, Q.Q.; Wu, Y.H.; Bing, H.J.; Zhou, J.; Wang, J.P. Vegetation Type rather than Climate Modulates the Variation in Soil Enzyme Activities and Stoichiometry in Subalpine Forests in the Eastern Tibetan Plateau. *Geoderma* **2020**, *374*, 114424. [CrossRef]
23. Beule, L.; Lehtsaar, E.; Corre, M.D.; Schmidt, M.; Veldkamp, E.; Karlovsky, P. Poplar Rows in Temperate Agroforestry Croplands Promote Bacteria, Fungi, and Denitrification Genes in Soils. *Front. Microbiol.* **2019**, *10*, 3108. [CrossRef]
24. Reis dos Santos Bastos, T.; Anjos Bittencourt Barreto-Garcia, P.; de Carvalho Mendes, I.; Henrique Marques Monroe, P.; Ferreira de Carvalho, F. Response of Soil Microbial Biomass and Enzyme Activity in Coffee-Based Agroforestry Systems in a High-Altitude Tropical Climate Region of Brazil. *Catena* **2023**, *230*, 107270. [CrossRef]
25. Clivot, H.; Petitjean, C.; Marron, N.; Erwin, D.; Genestier, J.; Blaszczyk, N.; Santenoise, P.; Laflotte, A.; Piutti, S. Early Effects of Temperate Agroforestry Practices on Soil Organic Matter and Microbial Enzyme Activity. *Plant Soil* **2020**, *453*, 189–207. [CrossRef]

26. López, R.E.I.; Navarrete, E.F.C.; Rosado, J.T.P.; García, C.R.S.; Margenot, A.J. Soil Nitrogen Cycling under Contrasting Management Systems in Amazon *Coffea canephora* Agroecosystems. *Soil Sci. Soc. Am. J.* **2021**, *85*, 1634–1648. [CrossRef]
27. Wang, F.Y.; Zhang, X.M.; Wei, M.T.; Wang, Y.; Liang, Z.S.; Xia, P.G. Appropriate Crop Rotation Alleviates Continuous Cropping Barriers by Changing Rhizosphere Microorganisms in *Panax notoginseng*. *Rhizosphere* **2022**, *23*, 100568. [CrossRef]
28. Zhang, L.Q.; Ji, W.X.; Yin, J.M.; Zhao, J.C.; Xin, Z.; Rao, D.M.; Meng, F.G.; Cui, J.H.; Zhang, W.; Zhao, H.Y. Long-Term Maize-Soybean Crop Rotation: Impacts on Soybean Yield, Soil Microbiota and Nitrogen Dynamics. *Front. Plant Sci.* **2025**, *16*, 1658885. [CrossRef]
29. Liu, M.X.; Hu, Z.H.; Fan, Y.; Hua, B.; Yang, W.; Pang, S.; Mao, R.; Zhang, Y.; Bai, K.Y.; Fadda, C.; et al. Effects of Leguminous Green Manure–Crop Rotation on Soil Enzyme Activity and Stoichiometry. *J. Plant Ecol.* **2024**, *17*, rtae065. [CrossRef]
30. McDaniel, M.D.; Grandy, A.S.; Tiemann, L.K.; Weintraub, M.N. Eleven Years of Crop Diversification Alters Decomposition Dynamics of Litter Mixtures Incubated with Soil. *Ecosphere* **2016**, *7*, e01426. [CrossRef]
31. Yu, H.; Wang, F.H.; Shao, M.M.; Huang, L.; Xie, Y.Y.; Xu, Y.X.; Kong, L.R. Effects of Rotations with Legume on Soil Functional Microbial Communities Involved in Phosphorus Transformation. *Front. Microbiol.* **2021**, *12*, 661100. [CrossRef]
32. Li, T.; Li, G.R.; Lu, Z.Q.; Zhao, D.Q.; Li, Y.Z.; Wang, Z.T.; Wen, X.X.; Liao, Y.C. Crop Diversification Increases Soil Extracellular Enzyme Activities under No Tillage: A Global Meta-Analysis. *Soil Tillage Res.* **2024**, *235*, 105870. [CrossRef]
33. Wang, L.; Guo, S.; Ge, T.; Mancl, K.M.; Hijri, M.; Iseri, Y.; Lee, S.J.; Feng, S.; Wang, L.; Ji, H.; et al. Plastic Mulch Productivity-Sustainability Tradeoffs and Pathways toward an Eco-Friendly Framework: Insights from a Global Meta-Analysis. *Nat. Commun.* **2026**, *17*, 1924. [CrossRef]
34. Yuan, Y.; Jianqiang, L.; Bo, Y.; Linling, W.; Wenqi, T.; Lianling, C. Influence of Root Secretions of Understory Chinese Herbal Medicines on the Characterization of Inter-Root Microbial Communities. *Front. Plant Sci.* **2026**, *16*, 1697347. [CrossRef]
35. Liao, J.J.; Dou, Y.X.; Wang, B.R.; Gunina, A.; Yang, Y.; An, S.S.; Chang, S.X. Soil Stoichiometric Imbalances Constrain Microbial-Driven C and N Dynamics in Grassland. *Sci. Total Environ.* **2024**, *924*, 171655. [CrossRef]
36. Abay, P.; Gong, L.; Luo, Y.; Zhu, H.Q.; Ding, Z.L. Soil Extracellular Enzyme Stoichiometry Reveals the Nutrient Limitations in Soil Microbial Metabolism under Different Carbon Input Manipulations. *Sci. Total Environ.* **2023**, *913*, 169793. [CrossRef]
37. Wang, Z.C.; Zhou, M.Y.; Liu, H.; Huang, C.; Ma, Y.H.; Ge, H.X.; Ge, X.; Fu, S.L. Pecan Agroforestry Systems Improve Soil Quality by Stimulating Enzyme Activity. *Peer J.* **2022**, *10*, 12663. [CrossRef]
38. Liu, H.H.; Ren, T.T.; Liao, J.H.; Chen, H.Y.H.; Zou, X.M.; Ruan, H.H. Nitrogen Deposition Alleviates Phosphorus-Induced Imbalances in Soil Enzyme Stoichiometry. *Commun. Earth Environ.* **2025**, *7*, 88. [CrossRef]
39. Wang, C.Q.; Jiao, R.Z. Adaptive Pathways Of Microorganisms to Cope with the Shift from P- to N-Limitation in Subtropical Plantations. *Front. Microbiol.* **2022**, *13*, 870667. [CrossRef]
40. Liu, C.H.; Wang, B.R.; Zhu, Y.Z.; Qu, T.T.; Xue, Z.J.; Li, X.Y.; Zhou, Z.C.; An, S.S. Eco-Enzymatic Stoichiometry and Microbial Non-Homeostatic Regulation Depend on Relative Resource Availability during Litter Decomposition. *Ecol. Indic.* **2022**, *145*, 109729. [CrossRef]
41. Luo, X.Z.; Hou, E.Q.; Chen, J.Q.; Li, J.; Zhang, L.L.; Zang, X.W.; Wen, D.Z. Dynamics of Carbon, Nitrogen, and Phosphorus Stocks and Stoichiometry Resulting from Conversion of Primary Broadleaf Forest to Plantation and Secondary Forest in Subtropical China. *Catena* **2020**, *193*, 104606. [CrossRef]
42. Wang, L.; Guo, S.; Hijri, M.; Farooq, M.; Rehman, A.; Ge, T.; Feng, S.; Wei, Z.; Zhang, J.; Zhao, C.; et al. Enhancing Carbon Restoration and Ecosystem Resilience in Global Drylands via Water-to-Carbon Biotransformation Strategies. *Commun. Earth Environ.* **2025**, *6*, 916. [CrossRef]
43. Shao, X.; Yang, W.; Wu, M. Seasonal Dynamics of Soil Labile Organic Carbon and Enzyme Activities in Relation to Vegetation Types in Hangzhou Bay Tidal Flat Wetland. *PLoS ONE* **2015**, *10*, 0142677. [CrossRef]
44. Fu, L.C.; Ding, Z.J.; Tang, M.; Zeng, H.; Zhu, B. Seasonal Dynamics of Activities, Temperature Sensitivities and Vector Characteristics of Extracellular Enzymes in Rhizosphere and Bulk Soils of Two Temperate Forests in Mt. Dongling, Beijing. *Acta Sci. Nat. Univ. Pekin.* **2022**, *58*, 503–516.
45. Schaap, K.J.; Fuchslueger, L.; Quesada, C.A.; Hofhansl, F.; Valverde-Barrantes, O.; Camargo, P.B.; Hoosbeek, M.R. Seasonal Fluctuations of Extracellular Enzyme Activities Are Related to the Biogeochemical Cycling of C, N and P in a Tropical Terra-Firme Forest. *Biogeochemistry* **2023**, *163*, 1–15. [CrossRef]
46. Nannipieri, P.; Trasar-Cepeda, C.; Dick, R.P. Soil enzyme activity: A Brief History and Biochemistry as a Basis for Appropriate Interpretations and Meta-Analysis. *Biol. Fertil. Soils* **2018**, *54*, 11–19. [CrossRef]
47. Zhao, Y.Z.; Liang, C.F.; Shao, S.; Chen, J.H.; Qin, H.; Xu, Q.F. Linkages of Litter and Soil C:N:P Stoichiometry with Soil Microbial Resource Limitation and Community Structure in a Subtropical Broadleaf Forest Invaded by Moso bamboo. *Plant Soil* **2021**, *465*, 473–490. [CrossRef]
48. Gao, P.Z.; Zhu, J.J.; Yang, K.; Yan, Q.L.; Zhang, J.X.; Yu, L.Z.; Diao, M.M.; Xu, S. Can Larch-Aralia Elata Agroforestry Systems Improve the Soil Chemical and Microbial Properties of Larch Plantations? *Agrofor. Syst.* **2022**, *96*, 885–896. [CrossRef]

49. Liu, Y.; Chen, Q.; Wang, Z.; Zheng, H.; Chen, Y.; Chen, X.; Wang, L.; Li, H.; Zhang, J. Nitrogen Addition Alleviates Microbial Nitrogen Limitations and Promotes Soil Respiration in a Subalpine Coniferous Forest. *Forests* **2019**, *10*, 1038. [CrossRef]
50. Weng, X.; Sui, X.; Liu, Y.; Yang, L.; Zhang, R. Effect of Nitrogen Addition on the Carbon Metabolism of Soil Microorganisms in a *Calamagrostis angustifolia* Wetland of the Sanjiang Plain, Northeastern China. *Ann. Microbiol.* **2022**, *72*, 18. [CrossRef]
51. Liu, M.; Gan, B.; Li, Q.; Xiao, W.; Song, X. Effects of Nitrogen and Phosphorus Addition on Soil Extracellular Enzyme Activity and Stoichiometry in Chinese Fir (*Cunninghamia lanceolata*) Forests. *Front. Plant Sci.* **2022**, *13*, 834184. [CrossRef]
52. Wang, C.; Yang, Q.; Zhang, C.; Zhang, X.; Chen, J.; Liu, K. Vegetation Restoration of Abandoned Cropland Improves Soil Ecosystem Multifunctionality through Alleviating Nitrogen-Limitation in the China Danxia. *Front. Plant Sci.* **2023**, *14*, 1116179. [CrossRef]
53. Yi, Z.; Xiao, X.; Zou, L.; Cen, C.; Shentu, X.; Yu, X.; Wang, W. From Environmental Signals to Adaptive Phenotypes: Signal-Responsive Regulation and Network Logic of Bacterial Small RNAs. *FEMS Microbiol. Rev.* **2026**, *50*, 41. [CrossRef]
54. Nieland, M.A.; Carson, C.M.; Floyd, V.; Zeglin, L.H. Product-Inhibition Feedbacks, Not Microbial Population Level Tradeoffs or Soil pH, Regulate Decomposition Potential under Nutrient Eutrophication. *Soil Biol. Biochem.* **2024**, *189*, 109247. [CrossRef]
55. Jiang, L.Z.; Ushio, M.; Imai, N.; Sugau, J.; Kitayama, K. Changes of Bacterial Versus Fungal Community Composition along a Forest Degradation Gradient of Logged-Over Tropical Rain Forests, and Their Consequences on Soil Enzyme Activities in Malaysian Borneo. *Plant Soil* **2024**, *510*, 541–563. [CrossRef]
56. You, Y.M.; Wang, J.; Huang, X.M.; Tang, Z.X.; Liu, S.R.; Sun, O.J. Relating Microbial Community Structure to Functioning in Forest Soil Organic Carbon Transformation and Turnover. *Ecol. Evol.* **2014**, *4*, 633–647. [CrossRef]

Disclaimer/Publisher's Note: The statements, opinions and data contained in all publications are solely those of the individual author(s) and contributor(s) and not of MDPI and/or the editor(s). MDPI and/or the editor(s) disclaim responsibility for any injury to people or property resulting from any ideas, methods, instructions or products referred to in the content.